Learning-based Virtual Inertia Control of an Islanded Microgrid with High Participation of Renewable Energy Resources

Norouzi, Mohammad Hossein ; Oshnoei, Arman; Mohammadi-Ivatloo, Behnam; Abapour, Mehdi

Published in:
IEEE Systems Journal

DOI (link to publication from Publisher):
10.1109/JSYST.2024.3370655

Publication date:
2024

Learning-based Virtual Inertia Control of an Islanded Microgrid with High Participation of Renewable Energy Resources

Mohammad Hossein Norouzi, *Member, IEEE,* Arman Oshnoei, *Member, IEEE,* Behnam Mohammadi-Ivatloo, *Senior Member, IEEE* and Mehdi Abapour *Member, IEEE*

***Abstract*—Renewable energy sources (RESs) are increasingly used to meet consumer demands in microgrids (MGs). However, high RES integration introduces system frequency stability, inertia, and damping reduction challenges. Virtual inertia (VI) control has been recognized as an effective solution to improve system frequency response in such circumstances. Conventional control techniques for virtual inertia control (VIC), which rely heavily on specific operating conditions, can lead to flawed performance during contingencies due to their lack of adaptivity. To address these challenges, this paper proposes a novel attitude found on brain emotional learning (BEL) to emulate virtual inertia and damping for effective frequency control. The BEL-based controller is capable of quickly learning and handling the complexity, non-linearity, and uncertainty intrinsic to the MGs, and it operates independently of prior knowledge of the system model and parameters. This characteristic enables the controller to adapt to various operating conditions, improving its robustness. The simulation results across three disturbance scenarios show that the proposed BEL-based controller significantly improves the system's response. The absolute maximum deviation of frequency was reduced to 0.0561 Hz in the final scenario, marking performance enhancements of 46.62% and 49.04% when compared with the artificial neural network (ANN)-based proportional-integral (PI) control and the standard proportional control, respectively. This underlines the controller's adaptability and superior effectiveness in varying operating conditions.**

***Index Terms*—Microgrid (MG) frequency control, Renewable energy sources (RESs), Virtual inertia control (VIC), brain emotional learning (BEL), artificial neural network (ANN), Proportional integral (PI) control**

NOMENCLATURE

Acronyms

ANFIS	Adaptive Neuro-Fuzzy Inference System
ANN	Artificial Neural Network
BEL	Brain Emotional Learning
BESS	Battery Energy Storage System
DFIG	Doubly Fed Induction Generator
DG	Distributed Generations
ESSs	Energy Storage Systems
EmS	Emotional Signal
GRC	Generation Rate Constraint
LFC	Load Frequency Control
MGs	Microgrids
MPC	Model Predictive Control
PI	Proportional-Integral
PV	Photovoltaic
RESs	Renewable Energy Sources
RoCoF	Rate of Change of Frequency
SyG	Synchronous Generator
SeI	Sensory Inputs
VD	Virtual Damping
VIC	Virtual Inertia Control
VSyG	Virtual Synchronous Generator

Parameters

β	Factor of frequency bias
K_{VI}	Virtual Inertia Emulator gain
T_g	Time constant of governor [s]
T_t	Time constant of Turbine [s]
T_{ESS}	Energy storage system constant [s]
D	System damping coefficient
H	System inertia
R	Droop constant
S	Apparent power [V.A]

Variables

ΔP_{th}	Output power change of Ggovernor [MW]
ΔP_{VI}	Inertia power [MW]
ΔP_{ESS}	Output power change of ESS [MW]
ΔP_{dist}	Output power change of disturbances [MW]
Δf	Frequency deviations [Hz]
ΔP_V	Output power change of PV [MW]
ΔP_W	Output power change of Wind [MW]

M. H. Norouzi, B.Mohammadi-Ivatloo, and M. Abapour are with the Department of Electrical and Computer Engineering, University of Tabriz,Tabriz 51666-16471,Iran. B.Mohammadi-Ivatloo is also with School of Energy, LUT University, Lappeenranta, Finland; (e-mails:mh.norouzi@ieee.org-&-hosseinnorouzi.77@gmail.com-bmohammadi@tabrizu.ac.ir-abapour@tabrizu.ac.ir)

A. Oshnoei is with the Department of Energy (AAU Energy), Aalborg University, 9220 Aalborg, Denmark; (e-mail:aros@energy.aau.dk)

I. INTRODUCTION

A. Background and Motivation

Currently, there is growing evidence that the inevitable effects of traditional power generation systems cannot be ignored [1]. To eliminate environmental problems such as greenhouse emissions and the lack of fossil fuel, these conventional generations can be replaced by renewable energy sources (RESs) [2]. Since there is a connection between the frequency of a system and the rotation speed and mass of the synchronous generators (SyGs), the frequency stability and the rotor speed regulation of the power grid generating units are connected [3]. Therefore, the microgrid (MG) infrastructure, which contains

TABLE I
THE COMPARISON BETWEEN THE EXISTING PAPERS AND THIS WORK

References	Model-free control	VI control method	ESS type	Considering damping properties	Control scheme
[7]	No	MPC	BESS	No	Not adaptive
[8]	No	H∞	BESS	No	Not adaptive
[9]	No	Derivative	BESS	Yes	Not adaptive
[10]	No	FOC	BESS&FC	Yes	Not adaptive
[13]	No	ANFIS	BESS&FC	No	Not adaptive
[16]	No	MPC	BESS	No	Not adaptive
[18]	No	H∞	BESS	No	Not adaptive
[20]	No	Derivative	BESS	No	Not adaptive
[21]	No	Derivative	BESS	No	Not adaptive
[23]	No	MPC	BESS	No	Not adaptive
[26]	No	Derivative	BESS	No	Not adaptive
[30]	No	MPC	BESS	Yes	Not adaptive
This study	**Yes**	**BEL**	**BESS**	**Yes**	**Adaptive**

energy storage systems (ESSs), wind and photovoltaic (PV) generation, and distributed generations (DGs), has shown to be a possible technique for reducing environmental concerns and solving the energy crisis issues [4]. To minimize the carbon intensity of electricity production, renewable energies have become vital, which brings stability problems in balancing the frequency response of the system [5]. However, the high presence of renewable energies declines the inertia significantly and brings more deviation in frequency or voltage of the system contrary to the conventional generation [6]. The use of inverters, acting as connectors between the grid and RESs, is a crucial factor in the decrease of inertia [3]. The dynamic stability of MGs under the high deployment of RESs remains a critical concern for current and future MG design [7]. A potential solution to address these stability problems involves using an inertia control structure that emulates virtual inertia (VI) power-based generation, thus enhancing system resiliency, operation, and stability [8]. Despite this potential solution, the topic is still under active research, with various strategies being investigated. The following section has reviewed the relevant literature to summarize the proposed solutions, their limitations, and opportunities for further exploration.

B. Literature Review

Several investigations have addressed the frequency control issue in low inertia MGs using ESSs equipped with VI support. In [7], VI control using model predictive control is provided for grid frequency stabilization in disturbance and uncertainty situations, but this controller has disadvantages like complex design and high cost. In [9], a VI control scheme based on a derivative method is used to improve the inertia and damping of the system to emulate the virtual damping (VD) and VI simultaneously and enhance the frequency stabilization of an islanded MG, which is proposed and successfully tested. Authors of [10] have proposed novel modeling of VI control that improves frequency stability, and also a fractional controller is presented as secondary control of the system. In [8] and [11], the authors have presented an extended virtual synchronous generator (VSyG) to make the frequency control of low inertia MGs robust in various disturbances and remove the unwanted effects of frequency measurements. In [12], an adaptive VI control method, operating without the need for communication, is proposed for the purpose of mitigating power oscillations in cascaded-type VSyGs. Supporting MG first frequency control using the VI in doubly fed induction generator (DFIG) and also adaptive neuro-fuzzy inference system (ANFIS)-based controller in the secondary control loop is investigated in [13]. Authors of [14] have ensured that implementing a special VSyG that emulates SyGs characteristics is an effective way of frequency control, regulating voltage amplitude in both operation modes of MGs. Authors of [15] and [16] have applied a model predictive control method to control the frequency of a multi-area interconnected power system considering nonlinear properties with high PV generation. In [17], an inverter-based VI control method is presented to achieve frequency control and MG stability, and dynamic impacts were also investigated. An H∞ controller is compared to an optimal proportional-integral (PI)-based VI control in [18] and demonstrates the effectiveness of the optimal controlling method. In [19], the authors have proposed a derivative method-depend on VI in the supercapacitor to regulate the MG frequency with different types of distributed energy resources. Refs. [19], [20], [21] and several published papers in this context overlook the effectiveness and importance of VD in the system's dynamic performance while adding this property to MGs is necessary for frequency stability and extending damping characteristics to MG. The comparison study between predictive control (MPC) and PI controlling methods using an MG's battery ESS to regulate and improve the frequency/voltage of the studied system is addressed in [22]. Authors of [23] presented the robustness and advantages of proposing an MPC control strategy against different parameters of an islanded MG. In [24], a two-stage controller design combines a tilt fractional-order integral derivative and a proportional derivative with filter controllers. This design, tuned by an artificial hummingbird algorithm, considers high RES penetration and EV integration in a two-area interconnected power system. In [25], a fractional-order controller-based VI control technique is suggested to facilitate frequency stabilization in multi-area power systems with high penetration of RESs. In [30], a two-layer multiple-MPC strategy is presented. This strategy manages an ESS equipped with VI control, aiming to address the load frequency control (LFC) problem in an isolated MG. A comparison

of the studied papers from different perspectives is provided in Table 1. Conforming to the aforementioned literature and Table 1, many previous studies have focused on improving control methods through the static derivative technique, aiming to reduce frequency fluctuations without considering damping properties and the VD technique. Also, previous research mainly developed model-based control approaches for VI, which heavily depend on the specific operating conditions, compromising their reliability and robustness.

C. Contributions

To fulfill this major gap, this paper suggests an innovative brain-emotional learning (BEL) approach designed to emulate virtual inertia and damping, thereby contributing to effective system frequency control. The suggested controller operates in a model-free manner, thereby controlling the VI loop without the required knowledge of the system's model and parameters. This feature bypasses any dependency of the control system on the specific operating point conditions. Essentially, it prevents the need for any preliminary knowledge of the system's parameters or structural configuration. A detailed simulation analysis is provided to establish the advantages of the presented control structure, especially under conditions of high RES penetration and load disturbances. The main contributions of this paper can be itemized as follows:

- Proposing a novel BEL-based approach for VI in MGs with high penetration of RESs. This approach enables the system to emulate virtual inertia and damping simultaneously for effective frequency regulation.
- Enhancement and improvement of the control system to handle complexities, non-linearity, and uncertainties associated with MGs. It indicates better adaptability to changes in parameters and fluctuations in loads.
- Providing comparative analysis to highlight the proposed controller's superior effectiveness and robustness against conventional techniques such as an ANN-PI controller and a proportional (P) control method.

D. Paper organization

This paper is classified as follows. Section 2 explains the frequency control process for the MG. The mathematical model for the BEL design is presented in section 3. Section 4 describes the ANN-based-controlling method. Section 5 delivers numerical simulations and arguments. Eventually, concluding remarks are provided in section 6.

II. Frequency Control in MGs

When a MG experiences an imbalance between consumption and generation, it can lead to frequency deviation, creating issues with frequency stability. This represents a significant challenge in the control, design, and operation of MGs [6]. In such situations, an inertia response, which is driven by the kinetic energy sourced from a generating unit, initially regulates the system's frequency for approximately 10 seconds [27]. To maintain an acceptable frequency during MG operation, a hierarchical control structure is necessary. This structure typically includes three distinct control loops: (1) an inertia control loop, (2) a primary control loop, and (3) a secondary control loop. These loops are designed to effectively reduce and overcome frequency deviation, as illustrated in Fig. 1[8]. Following a disturbance, the primary control attempts to stabilize the frequency within 10 to 30 seconds. Lastly, the secondary control, also known as LFC, restores the frequency to its appropriate bandwidth from 30 seconds to 30 minutes post-deviation [28].

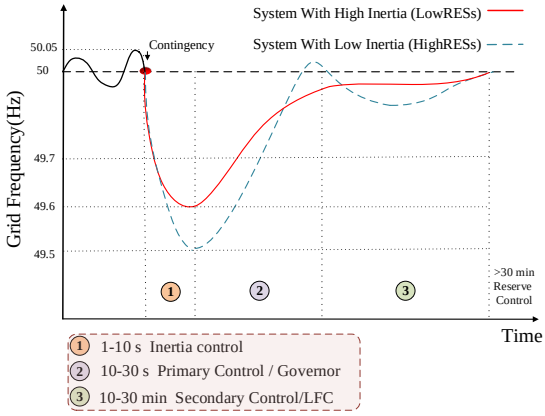

Fig. 1. Frequency response when a contingency occurs.

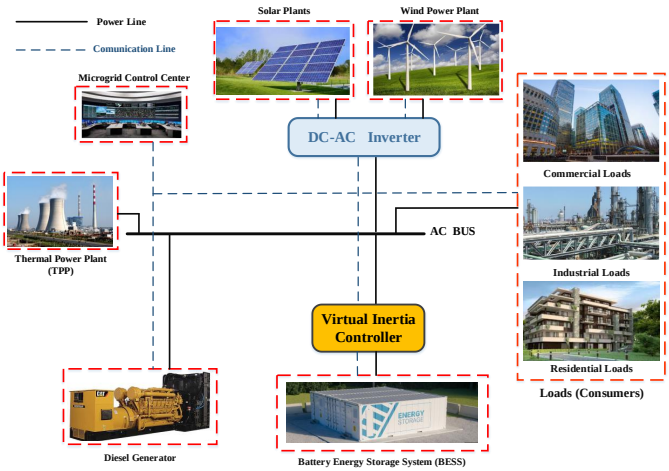

Fig. 2. The schematic of the studied system.

A. Dynamic Modeling of Studied MG

Traditional power generation systems that utilize conventional resources like coal and fossil fuels pose environmental hazards and fall short of meeting the increasing power demand [25]. Despite being gradually replaced by renewable energy units, these conventional units play an essential role in maintaining the inertia stability of the power system [29]. The studied MG, as illustrated in Fig. 2, comprises various generation units such as thermal, solar, and wind power plants along with diverse loads. This assortment helps to capture the multisource nature of the MG. The thermal power station is a traditional

power unit, with industrial and residential loads consuming the generated power. Furthermore, it's worth noting that wind farms and solar power plants are not equipped with inertia or damping controllers [10]. Consequently, integrating RESs into the MG, with their inherent probabilistic nature, changes the operating point, decreasing system inertia. This decline could impact the damping property, causing instability and frequency deviation in the MG [7]. A battery ESS (BESS) is introduced to address this issue. The BESS's ability to charge and discharge allows for the regulation of power discrepancies between generation and consumption within the initial 10 seconds. Furthermore, wind and solar power plants and loads are considered as disturbances because they introduce uncertainty into the system and do not contribute to frequency stabilization. According to Fig. 2, the control center sends the frequency fluctuations signal to the thermal power plant and VI control-based BESS via telecommunication joints. The mentioned signal, the BESS and thermal unit participate in the MG frequency regulation. A telecommunication network also exists, facilitating data and information exchange [10].

The mathematical structure of the studied MG is provided in Fig. 3. The governor nonlinear generation rate constraint (GRC) is used and assumed as 10% per minute [10]. The frequency deviation of the studied MG is calculated as:

$$\Delta f = \frac{1}{2Hs+D}(\Delta P_{th} + \Delta P_w + \Delta P_{PV} + \Delta P_{VI} - \Delta P_{load}) \tag{1}$$

where

$$\Delta P_{th} = (\frac{1}{1+sT_t})(\frac{1}{1+sT_g})(u - \frac{1}{R}\Delta f) \tag{2}$$

$$\Delta P_W = \frac{1}{1+sT_W}(\Delta P_{Wind}) \tag{3}$$

$$\Delta P_{PV} = \frac{1}{1+sT_{PV}}(\Delta P_{Solar}) \tag{4}$$

where ΔP_{th} is the generated power by the thermal power plant; ΔP_w denotes the power of the wind system; ΔP_{PV} is solar power change; ΔP_{VI} is the power change of VI-based ESS unit.

B. Virtual Inertia Control of MG

The VI is a specific manifestation of the VSyG. This concept was introduced as an emulation of the rotating mass inertia and damping properties of traditional SyG, owing to their effectiveness. Unlike the fixed inertia of a real SyG, VI provides superior performance and increased flexibility. It operates based on the rate of change of frequency (RoCoF) through an ESS, enhancing the system's stability and resilience [7].

By injecting extra active power into the system, VI reduces frequency deviations and improves stability. This way, RESs such as wind and solar plant units in the MG can effectively emulate the inertia typically provided by traditional units, further contributing to system stability [10]. The MG's inertia constant (H) is defined as:

$$H = \sum (HS_{SyG})/S_{MG} \tag{5}$$

where S_{SyG} denotes the power of the SyG, and S_{MG} indicates the power of the MG. The main idea of emulating rotating inertia is the derivative method which adds the ESS power to the system in case of contingencies. To reduce the sensibility of this technique to the noise, a low-pass filter is used in the system. The block diagram of this technique is illustrated in Fig. 4(a). The conventional VI is represented as:

$$\Delta P_{VI} = \frac{K_{VI}}{1+sT_{ESS}}(\frac{d(\Delta f)}{dt}) \tag{6}$$

where the K_{VI} is the gain of VI. The proposed VI control, depicted in Fig. 4(b), provides the VI and VD in low inertia and damping operations during the MG set-point value contingencies to improve the frequency response. The propounded VI control supplies emulations of damping properties and inertia simultaneously into the power system, which improves the stability and resiliency of the system and reduces frequency deviation in the case of high participation of RESs [16]. The VI and VD parts are used to modify the injected active power to the system and improve the time-based stabilization on the MG. Accordingly, the proposed intelligent method plays the supporter role of conventional generators. The proposed BEL-based VI control is represented as:

$$\Delta P_{VI} = (K_{VI}(\frac{d(u)}{dt}) + D_{VI}\Delta f)\frac{1}{1+sT_{ESS}} \tag{7}$$

where D_{VI} shows the VD of the proposed VI; and u is the generated control signal by the proposed BEL controller.

III. Brain Emotional Learning Controller Design

The BEL is considered as a model-free controller across various control engineering applications. Its quick learning capability makes it appropriate for robust and rapid decision-making in nonlinear systems, particularly those with inherent uncertainties. The controller comprises the Amygdala, responsible for emotional learning, the Orbitofrontal cortex, Sensory Cortex, and Thalamus. The model takes two inputs - Sensory Inputs (SeI) and Emotional Signal (EmS). The preprocessed signal from the Thalamus is received by the Sensory Cortex, which then forwards it to the Amygdala and Orbitofrontal Cortex. [31]. The output from the BEL is derived by taking the difference between the outputs from network A and network O, which is represented by:

$$u(t) = A(t) - O(t) \tag{8}$$

The SeI and EmS inputs are provided into Network A. The SeI input is then subjected to multiplication with a connection weight (M) to generate Network A's output, as illustrated by:

$$A(t) = SeI(t)M(t) \tag{9}$$

which $M(t)$ can changes as below:

$$M(t) = \int_0^t \delta m(t)dt + m(0) \tag{10}$$

where

$$\delta m(t) = \alpha SeI(t)[\max(0, EmS(t) - A(t) - A_a(t)] \tag{11}$$

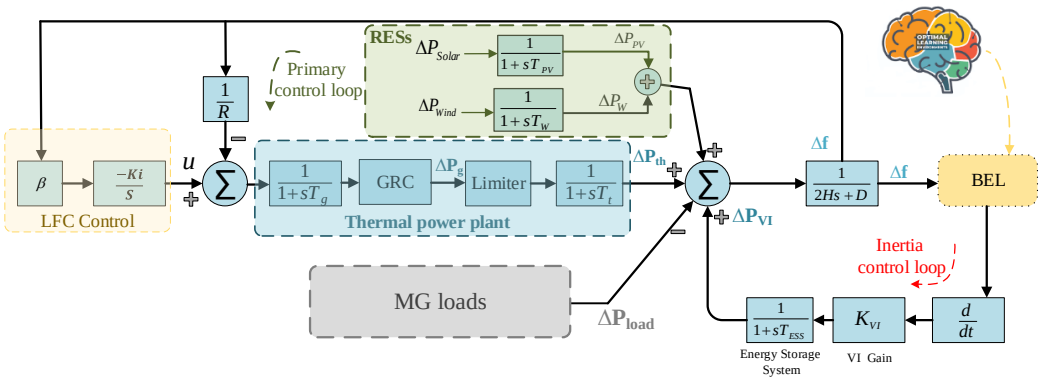

Fig. 3. Frequency response model of the MG.

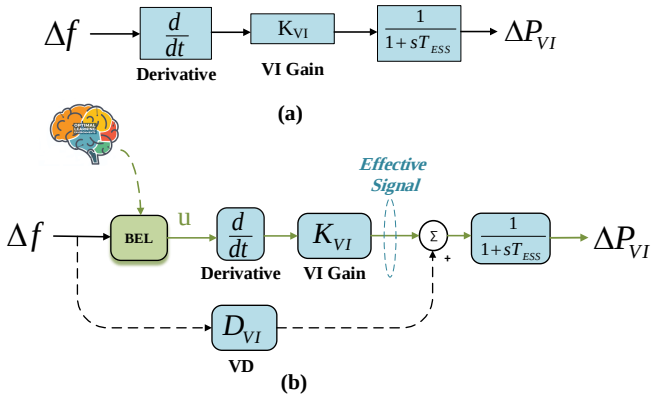

Fig. 4. VI control: (a) conventional, (b) proposed control structure

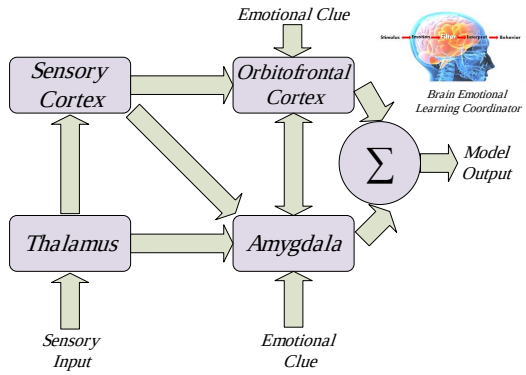

Fig. 5. BEL's Controlling Structure.

$$A_a(t) = \max[SeI(t)]M_a(t) \tag{12}$$

In this context, α represents the rate of learning; A_a denotes a neuron that directly gets the maximum sensory signals from the Thalamus; max[SeI] refers to the peak of all sensory signals [32]. The M_a can described as follows:

$$M_a(t) = \int_0^t \delta m(t)dt + M_a(0) \tag{13}$$

Network O receives inputs from SeI and EmS, along with the previous model output. The output of network O is calculated by multiplying the connection weight (N) with the SeI signal.

$$O(t) = SeI(t)N(t) \tag{14}$$

where N(t) changes as below:

$$N(t) = \int_0^t \delta n(t)dt + n(0) \tag{15}$$

where

$$\delta n(t) = \beta SeI(t)[A(t) - O(t) - EmS(t)] \tag{16}$$

where β is the inhibition rate; taking the initial states $m(0) = n(0) = M_a(0) = 0$ into consideration, the BEL output in (8) can be expressed as:

$$u(t) = SeI(t)[\alpha \int_0^t SeI(t)[max(0, EmS(t) - A(t) - A_a(t))]dt - \beta \int_0^t SeI(t)[A(t) - O(t) - EmS(t)]dt]. \tag{17}$$

To obtain the desired performance of BEL-based controller, it is vital to make a connection between SeI, EmS, and the controller's output (u) [33]. The SeI and EmS inputs are defined as below:

$$SeI = \phi_1 \Delta f + \phi_2 \int \Delta f dt \tag{18}$$

$$EmS = \gamma_1 \Delta f + \gamma_2 \int \Delta f dt + \gamma_3 u \tag{19}$$

where ϕ_1, ϕ_2 are the weighting coefficients for the SeI signal and γ_1,γ_2,γ_3 are the weighting coefficients for the EmS signal. These coefficients are determined via a trial-and-error process. The reason behind employing the SeI and EmS functions is to reach a rapid response, minimal overshoot and steady-state error, and minimal divergence from a reference point [34]. The proposed control scheme is illustrated in Fig. 5 and also the BEL's block diagram is depicted in Fig. 6 [32-34]. In this study, α and β are set at 0.86 and 0.98, respectively. These values are chosen to strike a balance between the learning rate

and the model's stability. Contrary to traditional controllers that are typically arranged for static operating conditions, the BEL method operates independently of such conditions and exhibits resilient performance against load disturbances and uncertainties [35].

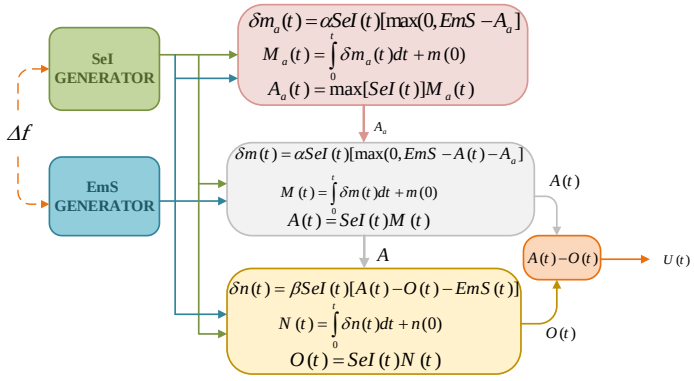

Fig. 6. Block diagram of proposed BEL controller.

IV. Artificial Neural Network Structure

The rationale for using the ANN method in this study originates from the limitations of a PI controller, particularly its performance being sensitive to fixed-tuned parameters. This implies that the controller maintains constant gains throughout all working conditions [36]. However, the dynamic tuning of controller gains amidst disturbances can be an effective strategy. This study, therefore, proposes an ANN-based approach to enhance the PI controller's capability. This method generates online supplementary gains for the PI controller in the VI control loop to maintain a fair comparison. The ANN technique adapts the PI controller to different changes in the MG, significantly speeding up the parameter adaptation. Input signals of the ANN-based tuning unit include the MG output and a fundamental data set. The primary objective of this approach is to minimize frequency deviation (Δf) under various MG operating modes. Hence, ANN generates appropriate set points, which are sent to the PI controller, ensuring MG stability under severe conditions [37]. The ANN, characterized by its inherently non-linear processing units or neurons, comprises three basic elements: weights $w_j = [w_{1j}, w_{2j}, ..., w_{nj}]$, an activation function $g(j)$, and a bias parameter φ. The activation function can take various forms, including sign, tangent sigmoid, and logarithmic sigmoid. The output of the hidden layer is computed based on the weighted input and bias, as mathematically represented in (20):

$$H_j = g\left(\sum_{i=1}^{n} w_{ij} y_i + \varphi\right) \qquad j = 1, 2, ..., L \tag{20}$$

Here, L denotes the hidden layer nodes.

Subsequently, the output of the output layer is computed as:

$$O_c = \sum_{j=1}^{L} H_j w_{jc} + \varphi \qquad c = 1, 2, ..., m \tag{21}$$

The goal of learning process is to make the mean squared error minimum, defined as:

$$E = \frac{1}{2}\sum_{r=1}^{N} (\Delta f - \Delta f_{ref})^2 \tag{22}$$

where N denotes the all samples; and Δf_{ref} signifies the reference frequency deviation, which is set to zero. The nonlinear neurons can update the of weight [38]. The ANN output layer holds two neurons corresponding to the control variables, namely the proportional and integral gains of the PI controller [39]. It is considered that the parameters of the gains of PI controllers are fixed and not able to overpass $\pm$ 0.4.

V. Simulation Results and Discussions

Various case studies are conducted to assess the performance of the proposed control scheme. The simulations are carried out using MATLAB/Simulink software. As illustrated in Fig. 2, industrial and residential loads wind turbine and PV are represented using the signal builder block. The thermal power plant's model employs first-order transfer functions, dead zone, and saturation blocks. The ESS is modeled using derivative, gain, and first-order transfer function blocks. The MATLAB/Simulink configuration parameters utilize a fixed-step solver to apply the studied LFC system with the suggested control loop. More information are given in [30]. A comparison study is done to study the effectiveness of the presented BEL controlling technique. To this end, the controller is compared to the ANN-based PI and P controllers. The parameters of the studied MG are given in Table II.

TABLE II
PARAMETERS OF STUDIED MG AND CONTROLLERS

Parameter	Value	Parameter	Value
f	60 Hz	T_{IN}	0.04s
T_{PV}	1.8s	T_{IC}	0.004s
T_{WTG}	1.5 s	T_{FC}	0.28s
T_g	0. 4s	T_t	0.01s
R	2.4 pu Hz/MW	T_{ESS}	0.1s
P	0.11	BEL (alpha-beta)	0.86-0.98
K_p	-10	K_i	0.86
K_d	0.591	λ	0.01
μ	0.3		

A. Step load change

In the first scenario, the system experiences a 30% step load change without the presence of PV and WT systems. The frequency response of the proposed BEL and ANN-based PI controller is illustrated in Fig. 7. From the figure, it can be observed that the BEL-based controller successfully minimized frequency deviation more effectively than the ANN-based PI controller. Quantitative error indices like the absolute maximum deviation (AMD) and settling time have been incorporated to assess frequency deviation. These results are presented in Table 3. It is notable that by leveraging the BEL-based controller, the AMD value of frequency has diminished to 0.15 Hz. Conversely, when the ANN-based PI is applied,

the AMD value remains at 0.1667 Hz. Stated differently, the proposed controller has offered a performance enhancement of 10.02% in comparison to the PI controller. The table shows the settling time value of fluctuations is the minimum while using the suggested control scheme . Fig. 8 shows the output power of the ESS when utilizing the BEL controller. It is evident from the figure that the ESS, controlled by the proposed method, charges and discharges more efficiently in response to the applied disturbance, compared to when the ANN-based PI controller controls the ESS.

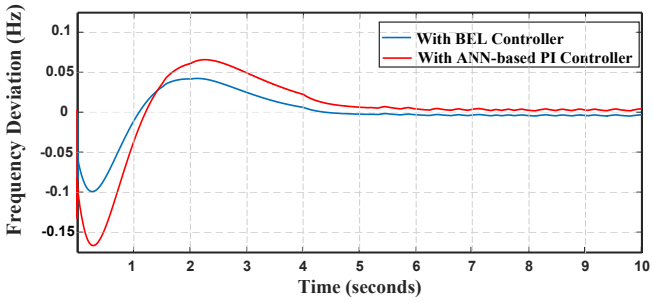

Fig. 7. Comparison of frequency responses of the MG with different controllers (first scenario).

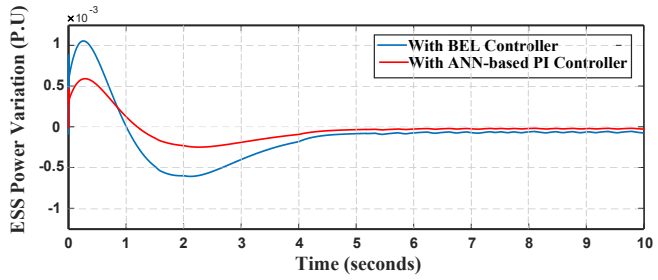

Fig. 8. ESS Power variation provided to the MG with different controllers (first scenario).

TABLE III
COMPARATIVE ANALYSIS OF THE PROPOSED CONTROLLER AND ANN-BASED PI CONTROL (FIRST SCENARIO).

Controller type	$\Delta f(Hz)$	Settling Time (s)
Proposed controller	0.15	4.4546
ANN-Based PI control	0.1667	7.3304

B. Sequence of step load changes

Fig. 9 (a)-(c) shows the application of a sequence of step load changes over a 200-second duration to the system, alongside the generation power of the PV and WT systems. Fig. 10 illustrates the performance of the proposed VI control under this scenario. It's noticeable that the BEL controller contributes more virtual inertia to the MG. The ESS power variation is shown in Fig. 11. The positive/negative variations in ESS power respectively indicate charge/discharge. More discharge from the ESS leads to an increase in the provision of virtual inertia to the MG. Peaks in deviation occur when unexpected changes in loads or RESs occur. The results suggest that the inertia loop, controlled by the BEL controller, delivers more power to the system, as shown in Fig. 10. It results in a better frequency performance compared to the ANN-based PI controller. Consequently, the implementation of the proposed VI control reduces transient excursion and provides additional virtual inertia, thereby enhancing the stability and robustness of the MG across various operational modes. For this scenario, frequency deviation assessment is also performed using AMD and settling time indices, as shown in Table IV which this analysis is based on the change in frequency that occurs at 155 s. It's highlighted that the BEL technique reduces the AMD rate of frequency to 0.0741 Hz, a 44.74% improvement over the ANN-based PI's 0.1341 Hz. Furthermore, the table indicates that the proposed control scheme achieves the shortest settling time.

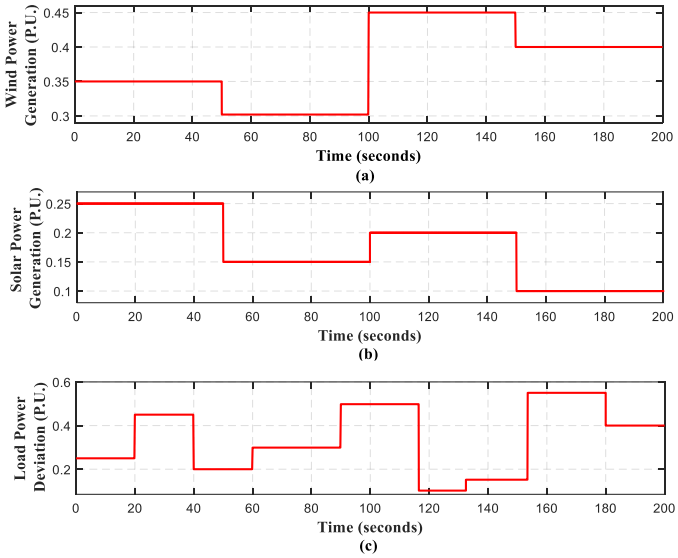

Fig. 9. Fluctuations in (a): wind system generation; (b): solar system generation; and (c): load power.

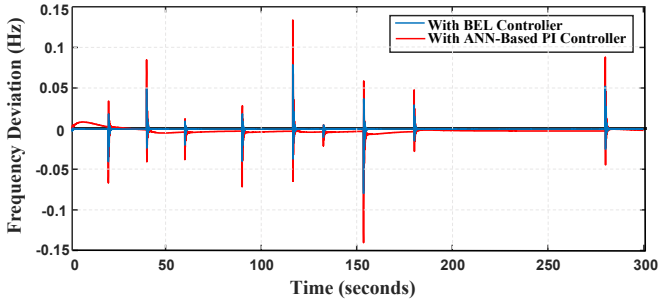

Fig. 10. Comparison of Frequency deviation in MG with different controllers (second scenario).

C. Random load change

Finally, in the last scenario, the effectiveness of the proposed learning-based VI control under the operation of MG with

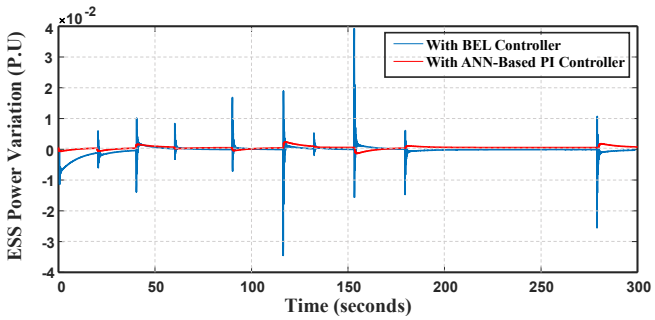

Fig. 11. ESS power variation with different controllers (second scenario).

TABLE IV
COMPARATIVE ANALYSIS OF THE PROPOSED CONTROLLER AND ANN-BASED PI CONTROL (SECOND SCENARIO).

Controller type	$\Delta f(Hz)$	Settling Time(s)
Proposed controller	0.0741	6.1539
ANN-Based PI	0.1341	26.7857

high penetration of PV and WT systems is fully tested. A P control method is also employed for comparison purposes, in addition to the ANN-based PI controller. This scenario presents an ordinary operating mode of the proposed MG with the participation of RESs and loads (consisting of residential and industrial). The generation power of wind and solar systems is shown in Fig. 13 (a) and (b), respectively. A severe load fluctuation of 800 s, as shown in Fig. 13 is considered.

The performance of proposed VI control is shown in Fig. 14 and 15.The inertia control method to stabilize the frequency of the MG is shown in this figure. Obviously, the suggested VI is more effective in minimizing the load fluctuations and mitigates the frequency deviations in comparison with other strategies. Similar to the previous two scenarios, key indicators of the AMD and settling time are used to assess frequency deviation, as presented in Table V which this analysis is based on the change in frequency that occurs at 180 s. The table illustrates that when the BEL-based controller is applied, the AMD value decreases to 0.0561 Hz. This indicates a performance improvement of 46.62% compared to an AMD value of 0.1051 Hz with the ANN-based PI, and an enhancement of 49.04% when compared to an AMD value of 0.1101 Hz with the standard P controller. Fig. 15 illustrates the variations in the output power of the ESS. It can be observed that the ESS when controlled by the proposed method, experiences a higher degree of charge/discharge in response to system disturbances compared to other approaches.

TABLE V
COMPARATIVE ANALYSIS OF THE PROPOSED CONTROLLER AND ANN-BASED PI CONTROL (THIRD SCENARIO).

Controller type	$\Delta f(Hz)$	Settling Time (s)
BEL	0.0561	9.8123
ANN-Based PI	0.1051	21.1376
P	0.1101	71.2831

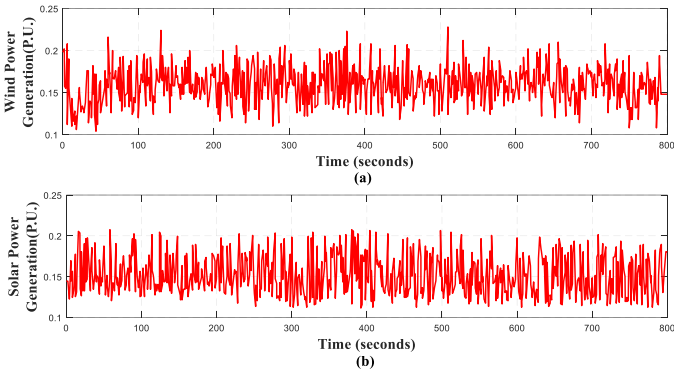

Fig. 12. The considered power disturbances of: (a) solar system and (b): wind system.

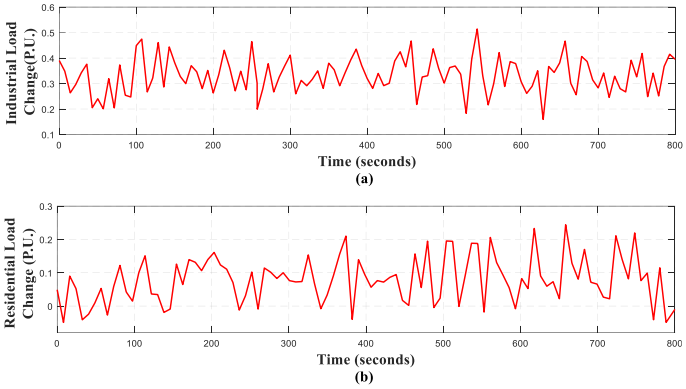

Fig. 13. The load deviations of studied MG (a): residential and (b): industrial.

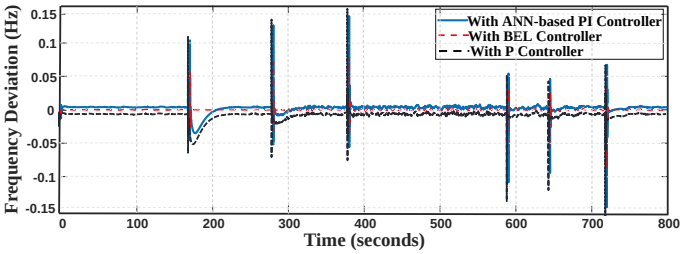

Fig. 14. Comparison of Frequency deviation in MG with different controllers (third scenario).

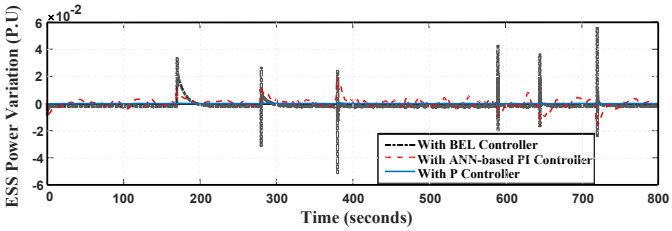

Fig. 15. ESS power variation with different controllers (third).

VI. CONCLUSION

This study presented a significant advancement in addressing frequency stability challenges in MGs with high integration

of RESs. A novel control strategy was implemented, applying a BEL-based VI control method, which demonstrated superior adaptability and robustness across diverse operating conditions. The system analysis highlighted critical parameters like the peak overshoot and undershoot of frequency deviations and the control of charging/discharging of the ESS. These parameters were key to comparing the dynamic performance of the proposed control method with other techniques. The main findings can be summarized as follows:

1) The BEL-based control strategy exhibited superior adaptability and robustness under various operating conditions.
2) Notably, the BEL-based controller reduced the AMD of frequency to 0.0561 Hz in the final scenario, indicating performance enhancements of 46.62% and 49.04% compared to ANN-based PI and standard P controllers, respectively.
3) The BEL-based controller demonstrated better control of ESS charging/discharging, thus contributing to more efficient utilization of the ESS unit.
4) The BEL-based controller proved more resilient in high RES penetration scenarios, demonstrating its robustness for various MG designs.

The effectiveness of the proposed controller provides a favorable basis for future research. Some potential directions include:

1) Expanding the application of the BEL-based VI control to multi-area interconnected MGs. This extension could reveal further benefits of the proposed controller in enhancing overall MG stability in high RESs integration scenarios.
2) Investigating the performance of the BEL-based VI control in more complex and dynamic MGs and power systems, where the interaction of multiple sources, loads, and storage devices further complicates the frequency control task.
3) Incorporating advanced machine learning techniques to improve the learning capability and responsiveness of the BEL-based controller, aiming for a more intelligent and self-adaptive control solution for future MGs.

REFERENCES

[1] N. Vafamand, M. M. Arefi, M. H. Asemani, and T. Dragicevic, "Decentralized Robust Disturbance-Observer Based LFC of Interconnected Systems," IEEE Trans. Ind. Electron., vol. 69, no. 5, pp. 4814–4823, 2022, doi: 10.1109/TIE.2021.3078352.

[2] A. Bakeer, G. Magdy, A. Chub, and H. Bevrani, "A sophisticated modeling approach for photovoltaic systems in load frequency control," Int. J. Electr. Power Energy Syst., vol. 134, no. June 2021, p. 107330, 2022, doi: 10.1016/j.ijepes.2021.107330.

[3] A. Fathi, Q. Shafiee, and H. Bevrani, "Robust frequency control of microgrids using an extended virtual synchronous generator," IEEE Trans. Power Syst., vol. 33, no. 6, pp. 6289–6297, 2018, doi: 10.1109/TPWRS.2018.2850880.

[4] T. Chen, J. Guo, B. Chaudhuri, and S. Y. Hui, "Virtual Inertia from Smart Loads," IEEE Trans. Smart Grid, vol. 11, no. 5, pp. 4311–4320, 2020, doi: 10.1109/TSyG.2020.2988444.

[5] M. Ahmed, G. Magdy, M. Khamies, and S. Kamel, "Modified TID controller for load frequency control of a two-area interconnected diverse-unit power system," Int. J. Electr. Power Energy Syst., vol. 135, no. July 2021, p. 107528, 2022, doi: 10.1016/j.ijepes.2021.107528.

[6] S. Oshnoei, A. Oshnoei, A. Mosallanejad, and F. Haghjoo, "Novel load frequency control scheme for an interconnected two-area power system including wind turbine generation and redox flow battery," Int. J. Electr. Power Energy Syst., vol. 130, no. March, p. 107033, 2021, doi: 10.1016/j.ijepes.2021.107033.

[7] N. Sockeel, J. Gafford, B. Papari, and M. Mazzola, "Virtual Inertia Emulator-Based Model Predictive Control for Grid Frequency Regulation Considering High Penetration of Inverter-Based Energy Storage System," IEEE Trans. Sustain. Energy, vol. 11, no. 4, pp. 2932–2939, 2020, doi: 10.1109/TSTE.2020.2982348.

[8] T. Kerdphol, F. S. Rahman, M. Watanabe, and Y. Mitani, "Robust Virtual Inertia Control of a Low Inertia Microgrid Considering Frequency Measurement Effects," IEEE Access, vol. 7, pp. 57550–57560, 2019, doi: 10.1109/ACCESS.2019.2913042.

[9] T. Kerdphol, F. S. Rahman, M. Watanabe, Y. Mitani, D. Turschner, and H. P. Beck, "Enhanced Virtual Inertia Control Based on Derivative Technique to Emulate Simultaneous Inertia and Damping Properties for Microgrid Frequency Regulation," IEEE Access, vol. 7, pp. 14422–14433, 2019, doi: 10.1109/ACCESS.2019.2892747.

[10] S. Oshnoei, M. Aghamohammadi, S. Oshnoei, A. Oshnoei, and B. Mohammadi-Ivatloo, "Provision of frequency stability of an islanded microgrid using a novel virtual inertia control and a fractional order cascade controller," Energies, vol. 14, no. 14, 2021, doi: 10.3390/en14144152.

[11] A. Rafiee, Y. Batmani, F. Ahmadi, and H. Bevrani, "Robust Load-Frequency Control in Islanded Microgrids: Virtual Synchronous Generator Concept and Quantitative Feedback Theory," IEEE Trans. Power Syst., vol. 36, no. 6, pp. 5408–5416, 2021, doi: 10.1109/TPWRS.2021.3077768.

[12] L. Li, Y. Sun, Y. Liu, P. Tian, and S. Shen, "A communication-free adaptive virtual inertia control of cascaded-type VSyGs for power oscillation suppression," Int. J. Electr. Power Energy Syst., vol. 149, no. March, p. 109034, Jul. 2023, doi: 10.1016/j.ijepes.2023.109034.

[13] P. García, C. A. García, L. M. Fernández, F. Llorens, and F. Jurado, "ANFIS-Based control of a grid-connected hybrid system integrating renewable energies, hydrogen and batteries," IEEE Trans. Ind. Informatics, vol. 10, no. 2, pp. 1107–1117, 2014, doi: 10.1109/TII.2013.2290069.

[14] S. D'Arco, J. A. Suul, and O. B. Fosso, "A Virtual Synchronous Machine implementation for distributed control of power converters in SmartGrids," Electr. Power Syst. Res., vol. 122, pp. 180–197, 2015, doi: 10.1016/j.epsr.2015.01.001.

[15] Y. Jia, Z. Y. Dong, C. Sun, and K. Meng, "Cooperation-Based Distributed Economic MPC for Economic Load Dispatch and Load Frequency Control of Interconnected Power Systems," IEEE Trans. Power Syst., vol. 34, no. 5, pp. 3964–3966, 2019, doi: 10.1109/TPWRS.2019.2917632.

[16] T. Kerdphol, F. S. Rahman, and Y. Mitani, "Virtual inertia control application to enhance frequency stability of interconnected power systems with high renewable energy penetration," Energies, vol. 11, no. 4, 2018, doi: 10.3390/en11040981.

[17] H. Bevrani and J. Raisch, "On Virtual inertia Application in Power Grid Frequency Control," Energy Procedia, vol. 141, pp. 681–688, 2017, doi: 10.1016/j.egypro.2017.11.093.

[18] T. Kerdphol, F. S. Rahman, Y. Mitani, M. Watanabe, and S.Kufeoglu, "Robust Virtual Inertia Control of an Islanded Microgrid Considering High Penetration of Renewable Energy," IEEE Access, vol. 6, pp. 625–636, 2018, doi: 10.1109/ACCESS.2017.2773486.

[19] M. Hajiakbari Fini and M. E. Hamedani Golshan, "Determining optimal virtual inertia and frequency control parameters to preserve the frequency stability in islanded microgrids with high penetration of renewables," Electr. Power Syst. Res., vol. 154, pp. 13–22, 2018, doi: 10.1016/j.epsr.2017.08.007.

[20] E. Rakhshani and P. Rodriguez, "Inertia Emulation in AC/DC Interconnected Power Systems Using Derivative Technique Considering Frequency Measurement Effects," IEEE Trans. Power Syst., vol. 32, no. 5, pp. 3338–3351, 2017, doi: 10.1109/TPWRS.2016.2644698.

[21] T. Kerdphol, F. S. Rahman, Y. Mitani, K. Hongesombut, and S. Küfeoğlu, "Virtual inertia control-based model predictive control for microgrid frequency stabilization considering high renewable energy integration," Sustain., vol. 9, no. 5, 2017, doi: 10.3390/su9050773.

[22] D. T. Vedullapalli, R. Hadidi, and B. Schroeder, "Combined HVAC and Battery Scheduling for Demand Response in a Building," IEEE Trans. Ind. Appl., vol. 55, no. 6, pp. 7008–7014, 2019, doi: 10.1109/TIA.2019.2938481.

[23] T. T. Nguyen, H. J. Yoo, and H. M. Kim, "Analyzing the impacts of system parameters on MPC-based frequency control for a stand-alone microgrid," Energies, vol. 10, no. 4, 2017, doi: 10.3390/en10040417.

[24] M. Nour, G. Magdy, J. P. Chaves-Ávila, Á. Sánchez-Miralles, and F. Jurado, "A new two-stage controller design for frequency regulation of low-inertia power system with virtual synchronous generator," J. Energy Storage, vol. 62, no. December 2022, p. 106952, Jun. 2023, doi: 10.1016/j.est.2023.106952.

[25] R. Mandal and K. Chatterjee, "Design of a maiden synthetic inertia controller using super-capacitor energy storages and electric vehicles and real-time validation of the performance of the controller," J. Energy Storage, vol. 55, no. PB, p. 105559, 2022, doi: 10.1016/j.est.2022.105559.

[26] T. T. Nguyen, H. J. Yoo, and H. M. Kim, "Application of model predictive control to bess for microgrid control," Energies, vol. 8, no. 8, pp. 8798–8813, 2015, doi: 10.3390/en8088798.

[27] M. R. Chen, G. Q. Zeng, Y. X. Dai, K. Di Lu, and D. Q. Bi, "Fractional-order model predictive frequency control of an islanded microgrid," Energies, vol. 12, no. 1, 2019, doi: 10.3390/en12010084.

[28] A. Oshnoei, M. Kheradmandi, S. M. Muyeen, and N. D. Hatziargyriou, "Disturbance Observer and Tube-Based Model Predictive Controlled Electric Vehicles for Frequency Regulation of an Isolated Power Grid," IEEE Trans. Smart Grid, vol. 12, no. 5, pp. 4351–4362, 2021, doi: 10.1109/TSyG.2021.3077519.

[29] M. H. Norouzi, M. Gholami, and R. Noroozian, "A comprehensive study of optimal demand management for a distributed network with the EV charging stations," in 2023 8th International Conference on Technology and Energy Management (ICTEM), Feb. 2023, pp. 1–6. doi: 10.1109/ICTEM56862.2023.10084262.

[30] S. Oshnoei, MR. Aghamohammadi, S.Oshnoei, S. Sahoo, A. Fathollahi, MH. Khooban, "A novel virtual inertia control strategy for frequency regulation of islanded microgrid using two-layer multiple model predictive control," Applied Energy,vol. 343,no.9, 2023 doi:10.1016/j.apenergy.2023.121233

[31] M. D. Qutubuddin and N. Yadaiah, "Modeling and implementation of brain emotional controller for Permanent Magnet Synchronous motor drive," Eng. Appl. Artif. Intell., vol. 60, no. November 2016, pp. 193–203, 2017, doi: 10.1016/j.engappai.2017.02.007.

[32] R. Khezri, A. Oshnoei, A. Yazdani, and A. Mahmoudi, "Intelligent coordinators for automatic voltage regulator and power system stabiliser in a multi-machine power system," IET Gener. Transm. Distrib., vol. 14, no. 23, pp. 5480–5490, 2020, doi: 10.1049/iet-gtd.2020.0504.

[33] B. Debnath and S. J. Mija, "Adaptive Emotional-Learning-Based Controller: A Practical Design Approach for Helicopters with Variable Speed Rotors," IEEE Trans. Ind. Informatics, vol. 18, no. 2, pp. 1132–1141, 2022, doi: 10.1109/TII.2021.3078116.

[34] A. Oshnoei, O. Sadeghian, and A. Anvari-Moghadam,"Intelligent Power Control of Inverter Air Conditioners in Power Systems: A Brain Emotional Learning-Based Approach," in IEEE Transactions on power Systems,2022, doi:10.1109/TRWRS.2022.3218589

[35] M. S. O. Yeganeh, A. Oshnoei, N. Mijatovic, T. Dragicevic and F. Blaabjerg, "Intelligent Secondary Control of Islanded AC Microgrids: Abrain Emotional Learning-Based Approach," in IEEE Transactions on Industrial Electronics, vol.70,no.7,pp.6711-6723,july 2023,doi:10.1109/TIE.2022.3203677

[36] A. Escamilla-García, G. M. Soto-Zarazúa, M. Toledano-Ayala, E. Rivas-Araiza, and A. Gastélum-Barrios, "Applications of artificial neural networks in greenhouse technology and overview for smart agriculture development," Appl. Sci., vol. 10, no. 11, 2020, doi: 10.3390/app10113835.

[37] H. Sorouri, M. Sedighizadeh, A. Oshnoei, and R. Khezri, "An intelligent adaptive control of DC–DC power buck converters," Int. J. Electr. Power Energy Syst., vol. 141, no. December 2021, p. 108099, 2022, doi: 10.1016/j.ijepes.2022.108099.

[38] H. Bevrani, F. Habibi, and S. Shokoohi, ANN-based self-tuning frequency control design for an isolated microgrid, no. October 2020. 2012. doi: 10.4018/978-1-4666-2086-5.ch012

[39] A. A. Derbas, A. Oshnoei, M. A. Azzouz, A. S. A. Awad, F. Blaabjerg and A. Anvari-Moghaddam, "Adaptive Damping Control to Enhance Small-Signal Stability of DC Microgrids," in IEEE Journal of Emerging and Selected Topics in Power Electronics, vol.11, no.3, pp. 2963- 2978, June 2023, doi: 10.1109/JESTPE.2023.3236809.